Received: 30 May 2026 | Revised: 3 September 2026 | Accepted: 28 September 2026 | Published online: 20 October 2026

RESEARCH ARTICLE

Smart Wearable Technology
2026, Vol. 00(00) 1–13
DOI: 10.47852/bonviewSWT620210590

BON VIEW PUBLISHING

Frequency-Domain ECG Analysis Enables Single-Encounter Hypertension Staging and Early Myocardial Remodeling Detection: A Prospective 384-Patient Study

Sugandhi Gopal[1,*], Prabhavathi Bhat[2], V. J. Karthikeyan[3], Shasha Jumbe[4], Vishwateja Reddy[1] and V. Harish[1]

[1] *Carditek Medical Devices, India*

[2] *Sri Jayadeva Institute of Cardiovascular Sciences & Research, India*

[3] *Department of Cardiology, The University of Manchester, UK*

[4] *Level 42 AI, USA*

Abstract: Hypertension diagnosis typically requires repeated office blood pressure measurements over multiple visits. This prospective single-center study evaluated whether frequency-domain analysis of a single high-resolution 12-lead electrocardiogram (ECG) could detect hypertension, grade its severity, and identify spectral signatures consistent with early myocardial involvement in treatment-naïve adults. Three hundred and eighty-four consecutive patients underwent clinical evaluation and digital 12-lead ECG recording with the Sydäntek capacitive platform. Both blood pressure measurements and ECG recordings were obtained in the sitting position after 5 minutes of rest, and 15-second recordings were used for analysis. After excluding 43 recordings with inadequate signal quality, we included 341 patients in this study. We used fast Fourier transform analysis of precordial leads V1–V6 to derive a transparent regression-based composite index from centroid frequency, total power, and spectral resonance peak ratio. The index was validated against guideline-defined blood pressure categories using stratified 5-fold cross-validation. The composite index achieved 88% overall accuracy for four-category grading (weighted κ = 0.868) and a weighted Receiver operating characteristic–area under the curve (ROC-AUC) of 0.978. Binary classification of normal versus any hypertension achieved 95% accuracy, 99% sensitivity, and 89% specificity. Misclassifications occurred only between adjacent severity categories, and lateral precordial leads V4–V6 contributed most to discrimination. Frequency-domain ECG analysis of a single 15-second recording provides an interpretable, scalable method for single-encounter hypertension detection and severity staging. These findings should be interpreted as a single-center pilot evaluation, and we look forward to confirmation by independent multicenter studies.

Keywords: hypertension, frequency-domain ECG, fast Fourier transform (FFT), myocardial remodeling, early detection

1. Graphical Abstract Summary

Figure Legend: Hypertension-linked fast Fourier transforms and correlation with remodeling.

Left: Sydäntek wireless capacitive ECG device enabling high-resolution 12-lead digital acquisition in a single 15-second recording.

Center: Representative FFT power spectra (V1–V6). Normotensive spectra (green) show low amplitude with rapid decay; severe hypertension spectra (red) demonstrate elevated amplitude and sustained high-frequency energy, reflecting increased myocardial workload, stiffness, and loss of harmonic coherence.

Top Right: Average maximum magnitude (V4–V6). Values rise progressively across hypertension severity categories.

Bottom: Schematic of left-ventricular geometric progression. Early concentric remodeling (Stages 1–2) remains reversible; progression to concentric or eccentric hypertrophy (Stages 3–4) results in largely irreversible hypertension-mediated organ damage (HMOD). The "*X*" marks the critical intervention window.

2. Introduction

Hypertension is the leading modifiable risk factor for cardiovascular disease, affecting more than 1.3 billion adults worldwide and contributing to over 10 million deaths annually [1–3]. Current international guidelines mandate repeated office blood pressure measurements over multiple visits, often supplemented by

***Corresponding author:** Sugandhi Gopal, Carditek Medical Devices, India. Email: sugopal@carditek.com

© The Author(s) 2026. Published by BON VIEW PUBLISHING. This is an open access article under the CC BY License (https://creativecommons.org/licenses/by/4.0/).

ambulatory or home monitoring, to establish a formal diagnosis [2, 3]. While this approach ensures accuracy, it is logistically demanding, requires substantial patient cooperation, and results in poor treatment initiation and long-term compliance; only about 50% of diagnosed patients begin and maintain antihypertensive therapy [4]. A reliable surrogate marker that enables accurate diagnosis and severity staging in a single clinical encounter could substantially reduce diagnostic burden and facilitate earlier intervention.

Electrocardiography (ECG) has stood the test of time as one of the most enduring and trusted sciences in cardiology. For over a century, it has served as a steadfast companion to clinicians, simple, reliable, and universally accessible, from small clinics to advanced tertiary centers. Yet, despite its ubiquity, the information derived from conventional ECG design and analysis remains limited. Its strength lies in availability, not depth. Intuitively, we sense that if more intelligent systems could be built around the electrical signals of the heart, the ECG could evolve from a static tracing into a dynamic diagnostic platform. Such an evolution could enable earlier detection of subtle physiological changes in diseases like hypertension, transforming the ECG from a routine test into a gateway for precision cardiovascular diagnostics.

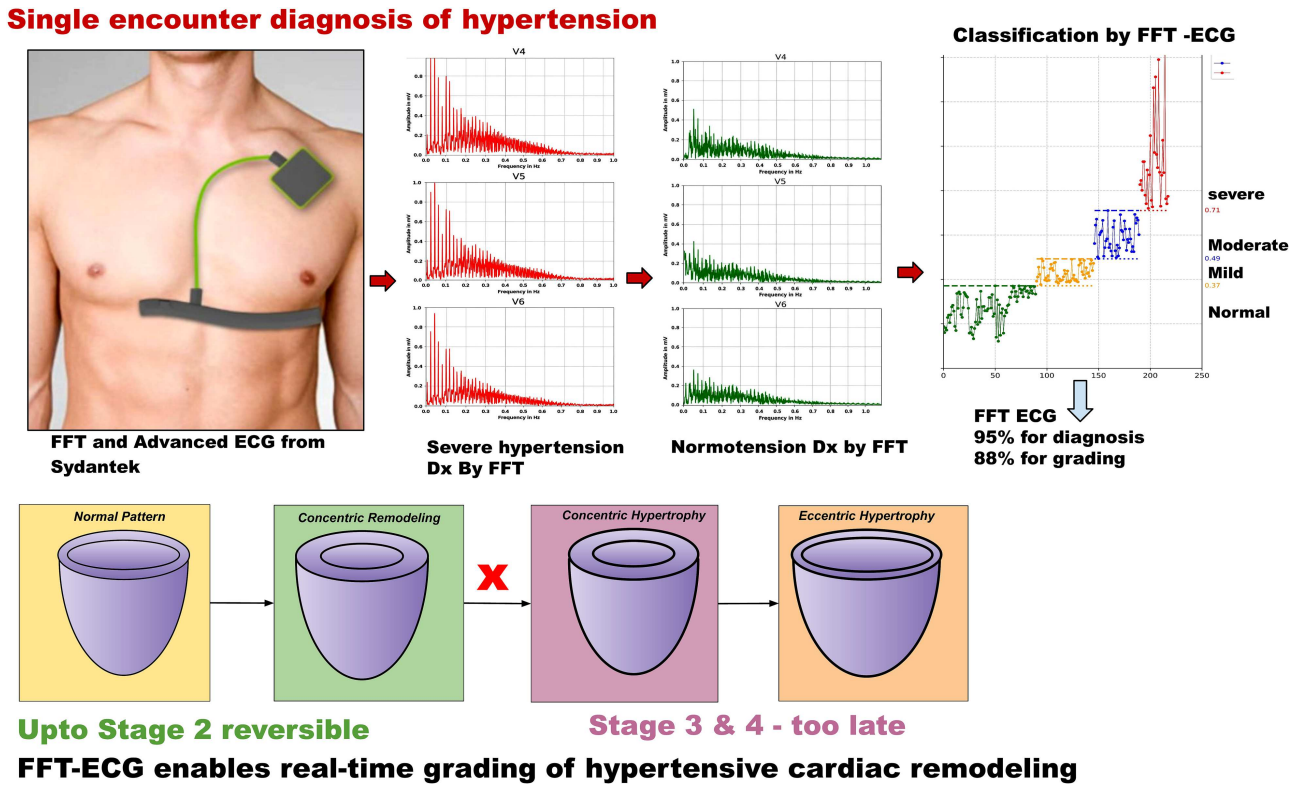
2.1. What is missing in time-domain ECG's and why does frequency-domain matter

Conventional electrocardiography, plotted in the time domain with time on the *x*-axis and amplitude on the *y*-axis, has been invaluable for more than a century in diagnosing major cardiac events such as myocardial infarction, ventricular hypertrophy, rhythm disturbances, and conduction abnormalities. Frequently overlooked even by trained physicians [5], yet in many conditions where myocardial fibers undergo subtle changes due to stretch and strain, conventional ECG remains insensitive unless extreme voltage shifts or ST-T changes occur within the 0–100 Hz range [6]. Early electrical alterations are often minute, comparable to a single instrument playing slightly off-note in a large orchestra, and are best detected through changes in frequency rather than amplitude.

The science of converting a regular ECG to a frequency-domain representation relies on the fast Fourier transform (FFT): we decompose the complex ECG waveform into a spectrum of sinusoidal components and quantify the power at each frequency. Instead of asking "what happens when?", frequency-domain analysis asks "which frequencies are present, and how strong are they?" [6]. This spectral perspective isolates subtle electrical variations that reflect myocardial stress, compliance, and tissue coherence. In a healthy ventricle, electrical activity is harmoniously organized; with progressive hypertension, myocyte hypertrophy, interstitial fibrosis, and impaired conduction disrupt this harmony, altering the spectral profile in predictable ways (Figure 1) [7–10]. Increased myocardial stretch and workload elevate total FFT power; reduced compliance shifts the centroid frequency upward; and fibrosis diminishes spectral resonance (SRPR%), reflecting loss of electrical coherence; the once-synchronized "orchestra" begins to sound discordant [7–10].

These spectral changes precede mechanical remodeling visible on echocardiography or MRI [7–10]. By identifying early electrical signatures of myocardial strain, frequency-domain ECG offers a window into disease at a potentially reversible stage, bridging the gap between electrical and mechanical diagnostics and redefining

Figure 1
Graphical abstract



how hypertension-mediated organ damage can be detected and monitored.

2.2. Analytic workflow and composite index derivation

These spectral features are integrated into a composite diagnostic index that balances sensitivity and specificity. By combining total power, centroid frequency, and SRPR%, the index captures both the magnitude and quality of myocardial electrical changes. This composite measure enables stratification of patients into early, intermediate, and advanced hypertensive remodeling stages, providing a reproducible framework for diagnosis and follow-up [7–10].

Importantly, different cardiovascular conditions manifest characteristic alterations within specific frequency bands of the ECG spectrum. Hypertensive myocardial remodeling predominantly affects lower-to-mid frequency bands (approximately 1.5–49 Hz), driven by increased wall stress, stiffness, and early fibrosis [7–10]. Other disease states such as ischemia, dyssynchrony, or infiltrative cardiomyopathies produce distinct spectral signatures that may appear in different subsets of the twelve standard ECG leads. This lead-specific variability provides valuable spatial information about regional myocardial involvement and electrical heterogeneity.

Because the hypertensive spectral band lies within the same frequency range as conventional ECG acquisition (< 50–60 Hz), these algorithms and feature-extraction methods can be seamlessly integrated into existing digital ECG systems without hardware modification [7–10]. This compatibility ensures that frequency-domain analysis can be implemented across standard clinical and wearable platforms, enabling scalable adoption for longitudinal monitoring and population-level screening.

The practical FFT workflow consists of the following steps:

1) Signal acquisition – Capture a clean, high-resolution ECG segment under resting conditions.
2) Pre-processing – Apply baseline correction and noise filtering to preserve physiological signal integrity.
3) Transformation – Use FFT to generate the power spectrum and quantify energy distribution across frequencies.
4) Feature extraction – Derive quantitative parameters such as total power, centroid frequency, maximum magnitude, and spectral resonance characteristics.
5) Composite index integration – Combine multi-band features into a unified diagnostic index for classification and risk stratification [7–10].

Because ECG analysis can yield a large number of potentially informative signal features, multi-feature integration is commonly used to improve classification performance [11]. While dozens of spectral features can be extracted from the ECG power spectrum, no single parameter is perfectly diagnostic because of overlap between adjacent severity categories. To address this, each feature is assigned a relative weight through feature-importance analysis (e.g., Random Forest importance scores), ensuring that the most discriminative spectral attributes contribute proportionally to the final model. The weighted features are then combined into a transparent, regression-based composite index that integrates total spectral power, centroid frequency, and spectral resonance characteristics into a single interpretable measure [12–16].

The present prospective study evaluated whether this composite spectral index derived from high-resolution 12-lead ECG frequency-domain analysis could accurately detect hypertension, grade severity across four clinically relevant categories, and identify spectral alterations associated with hypertension severity that may reflect early myocardial involvement in treatment-naive adults (Figure 2).

Figure 2 description: Comparison of time-domain ECG signals and fast Fourier transform (FFT) power spectra between normotensive and hypertensive subjects.

(a) Normotensive patient – Time-domain ECG: Conventional 12-lead time-domain ECG tracing from a normotensive patient showing standard voltage amplitudes and regular rhythm.

(b) Normotensive patient – FFT Frequency-domain spectrum: Corresponding FFT frequency-domain power spectrum (leads V1–V6) for the normotensive patient, displaying a concentrated spectral energy distribution with rapid amplitude decay across higher frequencies.

(c) Hypertensive patient – Time-domain ECG: Conventional 12-lead time-domain ECG tracing from a patient with moderate-to-severe hypertension displaying similar baseline voltage characteristics.

(d) Hypertensive patient – FFT Frequency-domain spectrum: Corresponding FFT frequency-domain power spectrum (leads V1–V6) for the hypertensive patient, demonstrating elevated amplitudes and broader spectral spread within the 1.5 to 49 Hz frequency range, particularly prominent in the mid-to-lateral precordial leads (V4–V6).

3. Methods

3.1. Study population

This prospective single-center cohort study was conducted in the outpatient department of a tertiary cardiology center. A total of 384 consecutive treatment-naive adults presenting for routine evaluation without any prior history of hypertension or antihypertensive medication use were recruited. All participants provided written informed consent. The study protocol was approved by the Institutional Ethics Committee of Sri Jayadeva Institute of Cardiovascular Sciences and Research (SJICR), Reference No: SJICR/EC/2020/028.

3.2. Clinical assessment and ECG acquisition

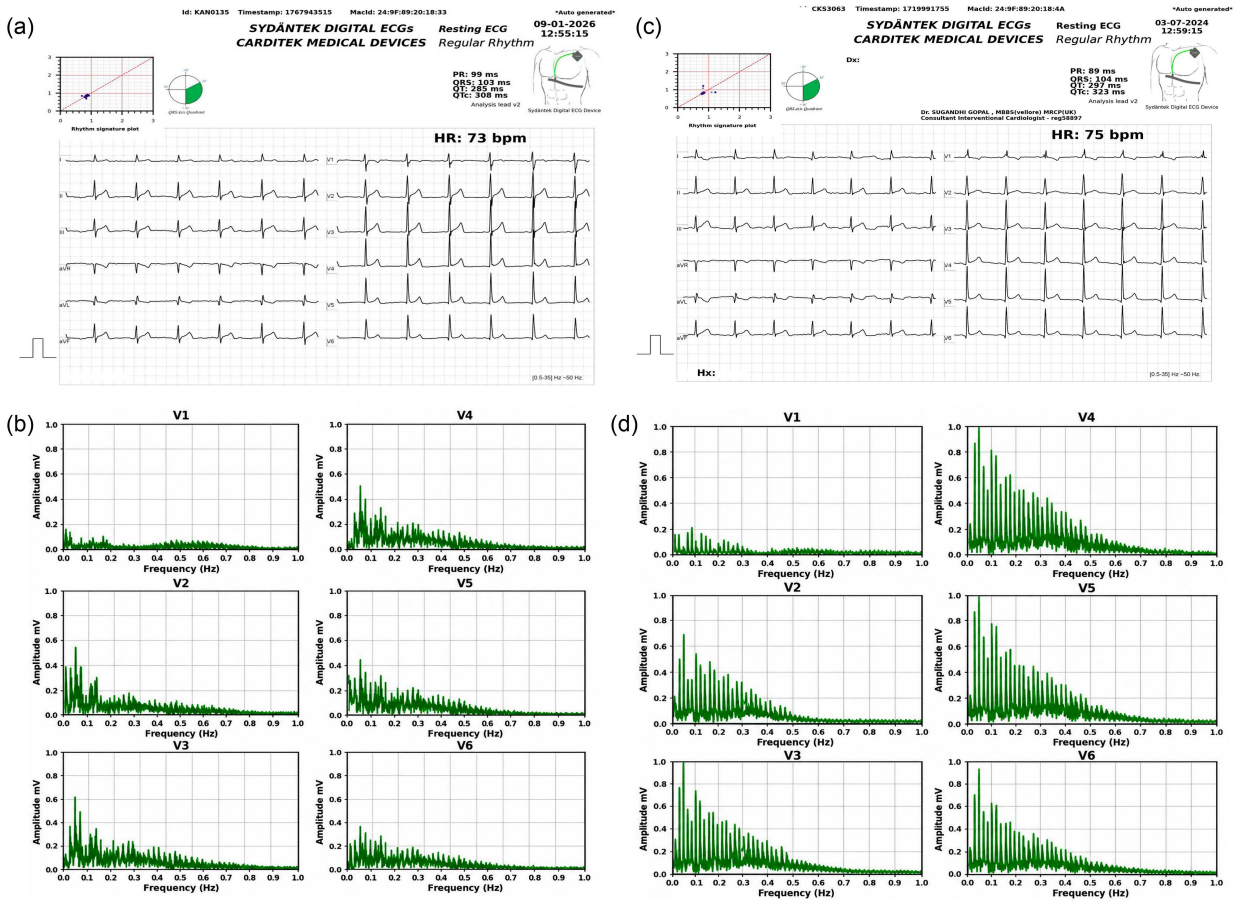
High-resolution 12-lead ECGs were recorded first in the sitting position. Only after completion of the ECG was office blood pressure measured in the sitting position according to current international guidelines, after 5 minutes of rest [17, 18]. Recent AI-enhanced ECG studies have also demonstrated the potential of ECG-derived features for hypertension detection and hypertension-related cardiovascular risk assessment [19]. Patients were then classified into guideline-defined hypertension categories.

3.3. Exclusion

Forty-three recordings (11.2%) were excluded because of inadequate signal quality in one or more precordial leads. Specific exclusion criteria were: (i) signal dropout or complete loss of usable signal; (ii) excessive noise or baseline artifact that precluded reliable frequency-domain analysis; or (iii) incomplete lead acquisition [20]. These exclusions occurred predominantly with the early prototype of the acquisition system; later recordings, after hardware and procedural refinements, showed exclusion rates below 1%. The final analyzed cohort comprised 341 patients.

Figure 2

Frequency-domain comparison of precordial ECG leads in normal versus moderate-to-severe hypertension. (a) Normotensive patient – Time-domain ECG; (b) Normotensive patient – FFT Frequency-domain spectrum; (c) Hypertensive patient – Time-domain ECG; (d) Hypertensive patient – FFT Frequency-domain spectrum



3.4. Frequency-domain ECG analysis

Precordial leads V1–V6 were subjected to FFT analysis. Canonical spectral surrogates were extracted: centroid frequency, total FFT power, and spectral resonance peak ratio (SRPR%). In addition, an expanded set of descriptors was calculated, including band-restricted power measures, normalized band power, multiple centroid definitions, resonance frequency metrics, and peak morphology features across the 1.5–90 Hz range. All features were computed using custom Python scripts based on scikit-learn and SciPy libraries [16].

3.5. Development and validation of the composite index

A transparent composite index was developed by integrating the canonical spectral surrogates and expanded descriptors. The process comprised four steps: (1) Feature extraction – the full set of spectral descriptors was extracted from each of the six precordial leads. (2) Feature weighting – relative importance of each descriptor was quantified using a Random Forest classifier (scikit-learn implementation, 500 trees). Feature-importance scores were derived from the mean decrease in Gini impurity. Lateral precordial leads (V4–V6) consistently ranked highest. (3) Composite index construction – retained features were combined into a single continuous score using a weighted linear combination. The weight assigned to each feature was proportional to its Random Forest importance score, normalized so that the sum of all weights equaled 1. (4) Validation – the composite index was evaluated against guideline-defined blood pressure categories using stratified 5-fold cross-validation [17, 18]. The overall analytical workflow is summarized in Table 1.

Table 1 description: The flowchart outlines a three-step analytical pipeline:

1) stratification of 341 treatment-naive patients into four blood pressure-based severity groups according to current international guidelines;

2) extraction of spectral ECG/FFT-ECG features including total power, SRPR%, maximum magnitude, and peak morphology metrics from high-resolution 12-lead digital recordings; and

3) concordance analysis using confusion matrices, overall classification accuracy, Cohen's kappa, and weighted kappa. This pipeline enables single-encounter hypertension staging from a 15-second ECG using spectral features not visible in conventional time-domain analysis.

4. Wearable Validation

All spectral indices and classification outputs were internally validated on recordings acquired using the Sydäntek ECG acquisition system. Validation focused on ensuring signal integrity

Table 1
Summary of methodology for spectral hypertension classification

Patient grouping by blood pressure	Spectral feature extraction	Concordance analysis
341 treatment-naive patients stratified into 4 categories • Normal: systolic blood pressure (SBP) <130 mmHg • Mild: SBP 130–139 or diastolic blood pressure (DBP) 80–89 mmHg • Moderate: SBP 140–159 or DBP 90–99 mmHg • Severe: SBP ≥160 or DBP ≥100 mmHg	High-resolution digital ECGs extract spectral parameters: • Total power (1.5-90 Hz) • Max magnitude • SRPR %, band power • Peak morphology metrics, etc.	Assessed using • Confusion matrix • Overall concordance rate • Cohen's kappa • Weighted kappa

and reproducibility within the dataset. Each recording was screened for electrical noise, verified across multiple time stamps, and processed only after confirming stable baselines and artifact-free segments [20].

5. Results

Age was not associated with hypertension grade, and body mass index (BMI) showed no monotonic relationship with severity. Male sex was more frequent in the higher blood pressure categories. These variables were not used as inputs to the spectral composite index.

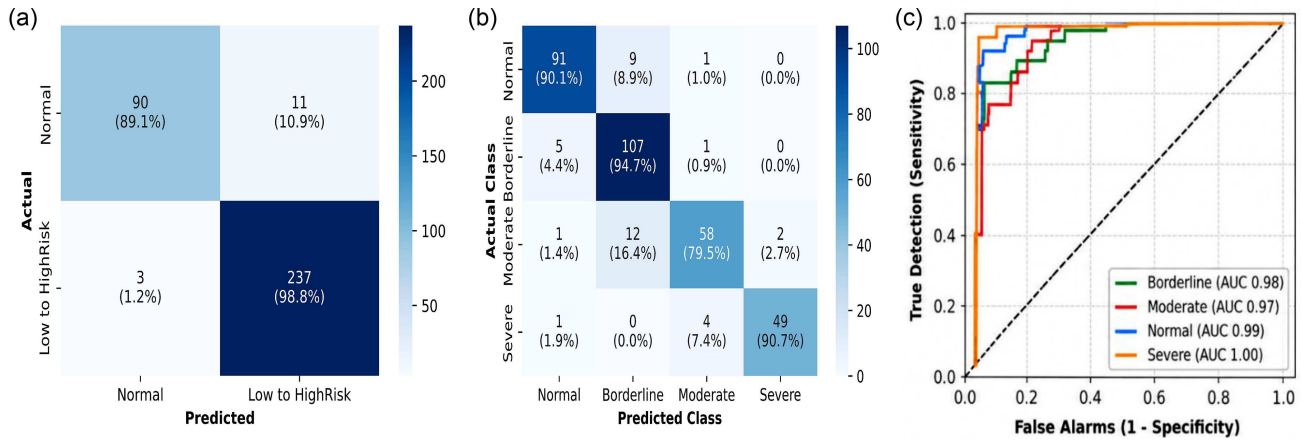
Of 384 consecutive treatment-naive adults recruited, 43 were excluded due to inadequate ECG lead quality (signal dropout, noise artifacts, or incomplete acquisition in one or more precordial leads), corresponding to an exclusion rate of 11.2%. These exclusions occurred predominantly during the initial phase of data acquisition with an early prototype of the Sydäntek device. Subsequent hardware refinements, optimized deployment procedures, and operator training substantially improved signal quality, with later datasets demonstrating exclusion rates below 1%.

Spectral analysis of the precordial leads V1–V6 demonstrated clear separation between normotensive and hypertensive cohorts (Figure 2). Canonical surrogates showed the expected physiological shifts: centroid frequency was higher, total FFT power was increased, and spectral resonance peak ratio (SRPR%) was reduced in hypertensive patients. Expanded spectral descriptors provided additional lead-specific granularity, with lateral precordial leads (V4–V6) contributing most to discrimination.

The regression-based composite index achieved 88% overall accuracy for grading hypertension severity across the four guideline-defined categories (Normal, Borderline/Mild, Moderate, Severe) with a weighted kappa of 0.868 (Table 2). Binary classification (normal vs any hypertension) yielded 95% accuracy, 99% sensitivity, 89% specificity, and a weighted Receiver operating characteristic–area under the curve (ROC-AUC) of 0.978 (Figure 3(a)). Misclassifications were limited to adjacent severity categories; no patient with severe hypertension was classified as normal, and no normotensive patient was classified as severe (Figure 3(b)). Individual class ROC-AUC values were 0.99 (normal), 0.98 (borderline), 0.99 (moderate), and 1.00 (severe) (Figure 3(c)). The primary performance estimates were obtained by stratified 5-fold cross-validation. Performance on a single held-out partition reached 92.75% accuracy; however, this figure is not presented as an independent external test-set result. The primary metrics remain those derived from 5-fold cross-validation.

The average maximum magnitude across leads V4–V6 increased progressively across hypertension severity categories (Figure 4(a)). Multivariate spectral feature space demonstrated

Figure 3
Diagnostic performance of the hypertension classification model evaluated by 5-fold cross-validation. (a) Cross-validation confusion matrix (5-fold) for binary classification; (b) comprehensive confusion matrix for all 341 patients (5-fold cross-validation); (c) diagnostic accuracy: ROC curves. (*n* = 341)



increasing separation between severity groups (Figure 4(b)). Class-specific discrimination was assessed using one-vs-rest ROC analysis (Figure 4(c)). Finally, comparison of individual spectral features with the combined model demonstrated improved classification performance with multi-feature integration (Figure 4(d)).

These findings demonstrate that frequency-domain ECG analysis can reliably quantify hypertensive remodeling and may serve as a scalable tool for early detection and longitudinal monitoring. Serial tracking of the composite spectral index across repeated visits demonstrated the potential utility of the score for longitudinal monitoring (Figure 5).

Figure 3 description:

(a) Cross-Validation confusion matrix (5-fold) Binary classification: Binary classification confusion matrix distinguishing normotensive patients (n = 101) from those with any degree of hypertension (borderline, moderate, or severe combined; n = 240). The model correctly identified 98.8% of hypertensive cases and 89.1% of normotensive cases. Only three hypertensive patients were misclassified as normal, and eleven normotensive patients were assigned to the hypertensive group, an asymmetry that favors clinical safety by minimizing missed diagnoses.

(b) Comprehensive confusion matrix-all 341 patients 5-fold cross validation: Four-category confusion matrix across the full severity spectrum (Normal, Borderline, Moderate, Severe). Correct classifications cluster along the diagonal, with accuracy exceeding 90% for both the Normal and Severe groups. "All misclassifications occurred between immediately adjacent categories for example, borderline assigned as normal or moderate assigned as borderline." No patient with severe hypertension was classified as normal, and no normotensive patient was classified as severe, confirming the model's gradient sensitivity and its suitability for clinical deployment.

(c) Diagnostic Accuracy: ROC Curves: Receiver operating characteristic curves generated by one-vs-rest analysis for each severity class. Area under the curve values were 1.00 for severe, 0.99 for normal, 0.98 for borderline, and 0.97 for moderate. All curves rise steeply toward the upper-left corner of the plot, reflecting high sensitivity at low false-positive rates. The dashed diagonal represents chance-level classification.

Figure 4

Comparative analysis of single-feature versus multi-feature spectral approaches for hypertension severity staging in 341 treatment-naive patients (a) Average v4-v6 max magnitude across categories; (b) t-SNE projection of FFT feature space {Class Separation}; (c) AUC Values by class; (d) Feature-wise classification accuracy comparison

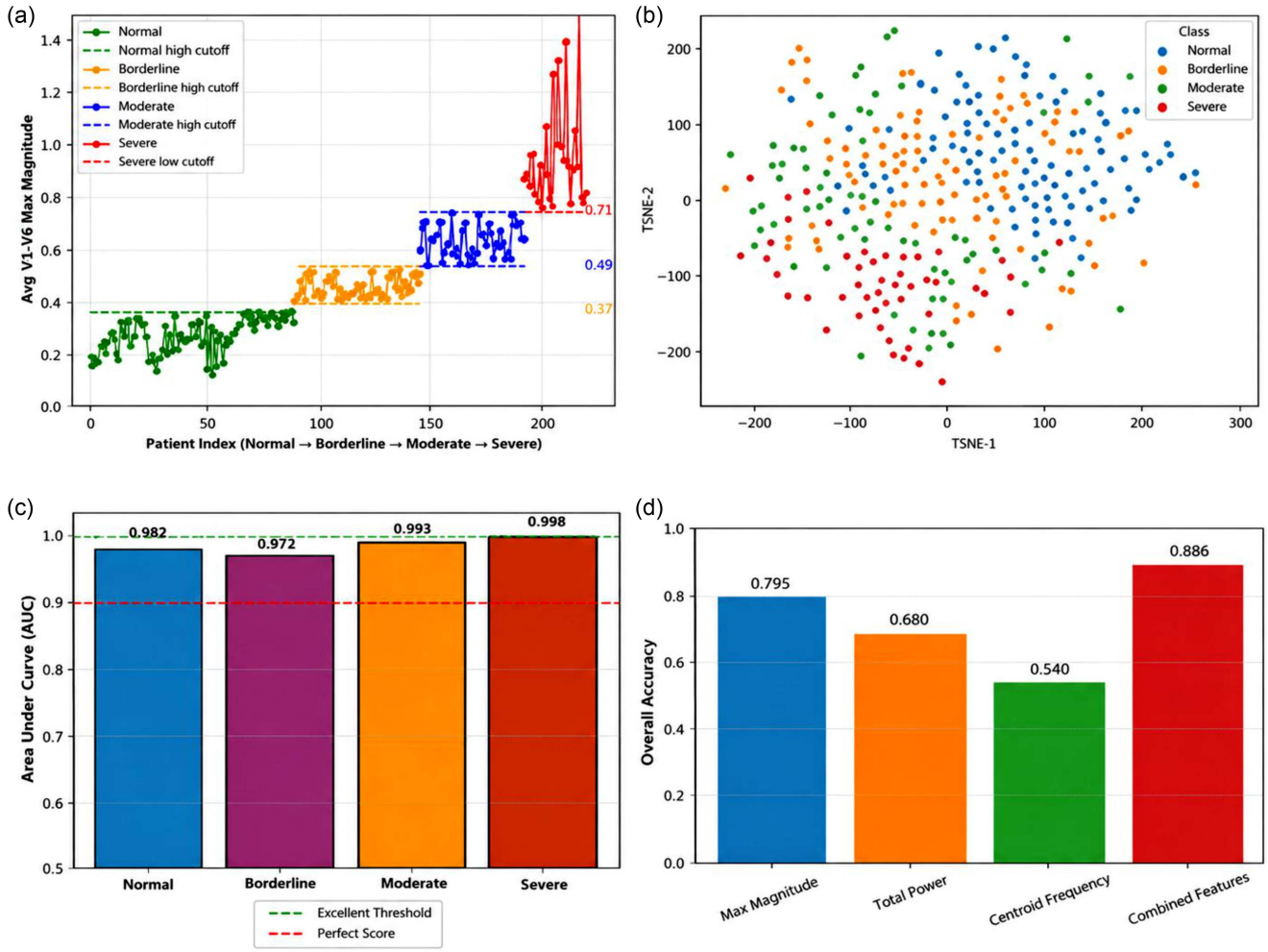


Figure 4 description:

(a) Average V4–V6 max magnitude across categories: Distribution of average maximum spectral magnitude across leads V4–V6, plotted for individual patients ordered by increasing hypertension severity (normal through severe). "A clear physiological gradient of apparent magnitude rises progressively" with worsening hypertension, reflecting increasing myocardial workload and wall stiffness. However, considerable overlap between adjacent groups, particularly in the borderline-to-moderate range (approximately 0.41–0.69), limits the utility of this single feature for precise multi-class staging. Dashed horizontal lines indicate the optimal single-feature classification thresholds identified at 0.41 (normal vs. borderline), 0.69 (borderline vs. moderate), and 0.73 (moderate vs. severe).

(b) *t*-SNE projection of FFT feature space (class separation): Two-dimensional *t*-SNE projection of the multi-feature FFT space, in which each point represents one patient colored by true hypertension class (blue: normal; orange: borderline; green: moderate; red: severe). The clear cluster separation, particularly between normal and severe groups, demonstrates that combining multiple spectral descriptors resolves the class overlap present with single-feature approaches, especially in the transitional borderline and moderate zones.

(c) AUC values by class: One-vs-rest ROC-AUC values for each hypertension severity class generated by the multi-feature Random Forest classifier. AUC values were 0.982 (normal), 0.972 (borderline), 0.993 (moderate), and 0.998 (severe), yielding a weighted average AUC of 0.978. Performance across all four classes substantially exceeds the conventional 0.90 threshold for excellent discrimination.

(d) Feature-wise classification accuracy comparison: Bar chart comparing overall classification accuracy across individual spectral features and the combined multi-feature model. Maximum magnitude alone achieved 79.5% accuracy; total power, 68.0%; and centroid frequency, 54.0%, the weakest single predictor, as frequency shifts in isolation lack sufficient discriminative context. Combining all spectral parameters within the Random Forest framework raised overall accuracy to 88.6%, a gain of 9-34 percentage points over any single feature, underscoring the diagnostic value of multi-band spectral integration.

Figure 5 description: Each row represents a single clinical visit. The color-coded bar spanning the four severity zones (Normal, Borderline, Moderate, Severe) is anchored by a vertical marker indicating the patient's composite spectral index score at that visit. The card is auto-generated directly from FFT feature data, requiring no manual scoring. Serial tracking across visits allows clinicians to visualize trajectory whether a patient is progressing toward higher-risk categories, stabilizing, or responding to intervention providing a practical framework for longitudinal hypertension monitoring and treatment compliance assessment.

Table 2 description: Performance metrics of the machine learning model for hypertension severity classification using FFT-derived spectral ECG features across 341 patients.

Compares performance from one held-out partition with the primary estimate obtained by stratified 5-fold cross-validation. The primary results are those from 5-fold cross-validation (accuracy 0.880, weighted κ = 0.868, ROC-AUC 0.978). The higher accuracy of 0.928 on a single partition is shown only for completeness and is not an independent external test-set result.

Per-class precision, recall, F1-score, and the distribution of adjacent-category misclassification are presented in Table 3.

Table 3 description: shows per-class precision, recall, and F1-score. Performance was strong across all categories, with particularly high precision for normal (0.96) and severe (0.89) cases. The overall weighted accuracy of 88% confirms the model's robustness as a multi-class staging tool; the moderate category showed the highest rate of adjacent misclassifications (n = 14), consistent with the physiological overlap inherent to transitional hypertensive states.

Figure 5
Patient-level hypertension risk scorecard generated from serial spectral ECG/FFT-ECG recordings across nine visits over a two-month period

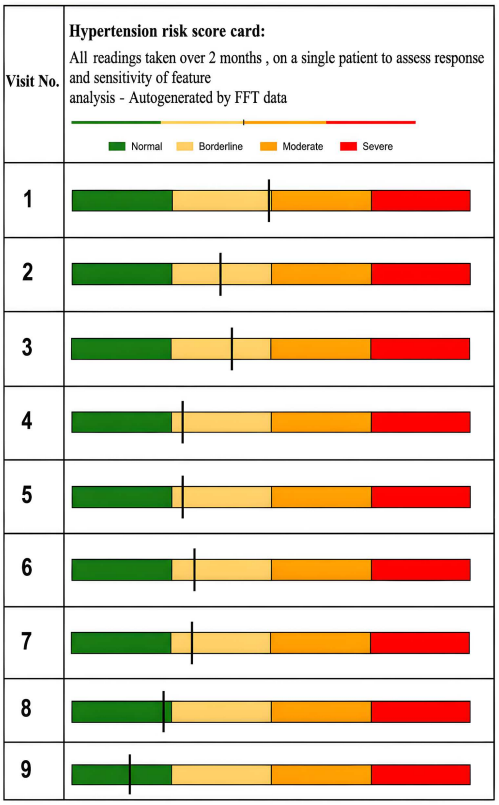


Table 2
Comprehensive classification report – 341 patients

Metric	Single held-out partition	Overall cross-validation
Total patients analyzed	341	341
Accuracy	0.9275	0.8798
Cohen's kappa	0.9007	0.8347
Weighted kappa	0.9322	0.8678
ROC-AUC	0.9855	0.9781
Macro F1-score	0.9263	0.8757
Weighted F1-score	0.9277	0.8789

6. Discussion

This prospective single-center study in 341 treatment-naive patients demonstrates that frequency-domain analysis of a single high-resolution 12-lead ECG enables accurate detection and severity staging of hypertension while identifying spectral signatures

Table 3
Final summary of FFT-based classification performance

Class	Precision	Recall	F1-score	Support (clinical classification)	FFT classification	Numbers misclassified into adjacent categories
Normal	0.96	0.89	0.92	101	90	9
Borderline	0.82	0.95	0.88	113	107	6
Moderate	0.87	0.74	0.80	73	58	14
Severe	0.89	0.91	0.90	54	49	4
Accuracy			0.88	341		
Macro Avg	0.89	0.87	0.88	341		
Weighted Avg	0.88	0.88	0.88	341		

consistent with early myocardial involvement. The transparent regression-based composite index achieved 88% overall accuracy for four-category grading (weighted κ = 0.868) (Table 4) and excellent binary performance (95% accuracy, 99% sensitivity, weighted ROC-AUC 0.978). Results were reproducible across recordings acquired using the Sydäntek wearable ECG platform, supporting the feasibility of spectral analysis in a wearable ECG setting.

A key strength of this work is the exclusively treatment-naive cohort, which eliminated confounding effects of antihypertensive therapy on myocardial structure and electrophysiology, a limitation common in many prior AI-ECG studies [10, 19]. The observed spectral changes (increased total FFT power, elevated centroid frequency, and reduced spectral resonance peak ratio) align with the underlying pathophysiology of hypertensive heart disease, including increased myocardial workload, stiffness, and early interstitial fibrosis. Lateral precordial leads (V4–V6) provided the strongest discriminative power, consistent with their anatomical proximity to the left ventricle (Figure 6). Importantly, in the borderline and mild hypertension subgroups, spectral changes were already present even when conventional time-domain ECG criteria and available echocardiographic assessments (when performed) showed no clear structural abnormalities. This observation supports the interpretation that frequency-domain analysis may detect electrical alterations that precede both standard ECG voltage criteria and overt structural remodeling.

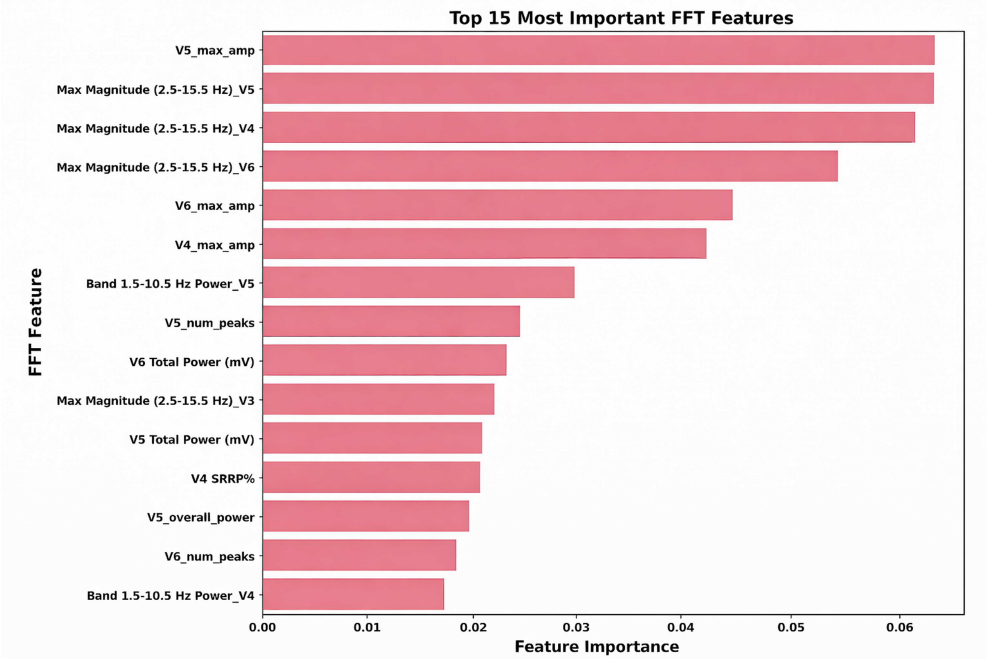
Figure 6 description: The horizontal bar chart displays the relative discriminative contribution of the 15 highest-ranking spectral features. Lateral precordial leads (V4–V6) dominate the ranking, with V5 maximum amplitude and band-limited maximum magnitude in the 2.5–15.5 Hz range occupying the top positions. Peak amplitude metrics across V4–V6 and band-restricted power in the 1.5–10.5 Hz range collectively account for the majority of the model's discriminative capacity. These features are physiologically coherent: the lateral precordial leads overlie the left-ventricular free wall, and the 1.–15.5 Hz band corresponds to the frequency range most sensitive to changes in myocardial wall stress, compliance, and early interstitial fibrosis associated with hypertensive remodeling.

Compared with recent AI-enhanced and deep-learning ECG studies demonstrating the potential of ECG-based approaches for hypertension detection, prediction, and identification of hypertension-mediated cardiac changes [10, 19], our approach demonstrated competitive performance while using an interpretable, transparent model rather than a black-box algorithm. Importantly, we extend beyond binary classification by successfully grading severity across four clinically relevant categories, with misclassifications confined to adjacent groups only. This ordinal reliability enhances clinical safety and utility.

Table 4
Summary of diagnostic performance and clinical significance of the spectral ECG/FFT-ECG classification pipeline

Performance metric	Finding	Clinical significance
Overall 4-class accuracy	88% (weighted κ 0.868)	Robust multi-class staging from a single 15-second recording
Binary accuracy (normal vs. any HTN)	95%	Supports frontline screening and triage
Sensitivity (binary)	99%	Minimizes missed high-risk cases; enhances clinical safety
Specificity (binary)	89%	Acceptable false-positive rate for a screening application
Weighted ROC-AUC	0.978	Excellent overall discrimination across all severity classes
Class-specific AUC	0.97–1.00 across all classes	Reliable performance even in transitional (borderline) category
Misclassification pattern	Adjacent categories only	Ordinal integrity preserved; no clinically dangerous cross-category errors
Model type	Transparent regression-based composite index (Random Forest weighting)	Interpretable and auditable; supports clinical adoption and shared decision-making

Figure 6
Feature-importance ranking derived from the Random Forest classifier applied to FFT spectral parameters across 341patients



The single-encounter nature of a 15-second recording addresses a major practical limitation of current hypertension guidelines, which require repeated blood pressure measurements over multiple visits [1–3]. By detecting spectral signatures of early reversible myocardial remodeling (Figure 4), this method opens a critical window for timely intervention.

7. Limitations

The study was conducted at a single tertiary center in India, which may limit generalizability across diverse ethnicities, age groups, and comorbidities. External multi-center validation is therefore required and is currently being planned. A strength of the present study is the exclusive recruitment of treatment-naive patients. Obtaining large numbers of adults who have never received antihypertensive therapy is difficult in contemporary clinical practice, yet this design eliminates the confounding effects of medication on myocardial structure and electrophysiology. While the single-center setting limits immediate generalization, the treatment-naive nature of the cohort enhances the physiological interpretation ability of the spectral findings. No systematic concurrent echocardiography or cardiac magnetic resonance imaging was performed for the full cohort. The inference that the observed spectral alterations reflect early hypertensive myocardial involvement is based on established pathophysiology and on the clinical observation that these changes were already progressive in the borderline and mild subgroups, where conventional ECG voltage criteria were generally absent and available echocardiographic assessments (when performed) showed no clear structural abnormalities. Formal imaging correlation remains necessary. Although the exclusive recruitment of treatment-naive patients removed the confounding influence of antihypertensive therapy, other potential confounders such as age, sex, BMI, diabetes, and heart rate were not subjected to formal multivariable adjustment. Residual confounding therefore cannot be excluded. The primary performance estimates are those obtained from stratified 5-fold cross-validation. The higher figure of 92.75% accuracy on a single held-out partition should not be interpreted as an independent external test-set result.

This study should be interpreted as a single-center pilot/proof-of-concept evaluation. External validation by independent clinical teams is the essential next step.

8. Conclusion

Frequency-domain ECG analysis using a transparent composite index offers a rapid, interpretable, and scalable single-encounter tool for hypertension detection and staging. This builds on our prior Sydäntek wearable validation studies [6–8]. This approach has strong potential to reduce diagnostic burden, improve risk stratification, and support timely intervention in the global management of hypertensive cardiovascular disease.

Table 4 description: The spectral composite index achieved AUC values exceeding 0.97 across all four hypertension severity classes, surpassing most published AI-ECG benchmarks for this diagnostic task. Sensitivity for severe hypertension reached 99%, ensuring reliable identification of patients requiring urgent clinical assessment. All misclassifications were confined to adjacent severity categories, preserving the ordinal structure of the staging framework and minimizing clinically significant errors. The transparent, regression-based model architecture facilitates clinical adoption in a way that black-box deep-learning systems cannot.

The principal clinical implications of these findings are summarized in Table 5.

Table 5 description: Spectral ECG/FFT-ECG analysis demonstrated high diagnostic accuracy across all hypertension severity categories (AUC >0.97) and strong binary classification performance, with 95% accuracy and 99% sensitivity for high-risk case detection. Agreement between FFT-based staging and blood pressure-defined severity was substantial (Cohen's kappa 0.82; weighted kappa 0.87), affirming that spectral indices reliably

Table 5
Summary of key clinical points arising from spectral ECG/FFT-ECG analysis

What this study shows	Why it matters clinically
AUC >0.97 across all hypertension severity classes	Exceeds most published AI-ECG benchmarks for hypertension detection
95% binary accuracy; 99% sensitivity for high-risk cases	Reliable frontline triage without requiring repeat blood pressure measurements
Cohen's *s* kappa 0.82; weighted kappa 0.87	Substantial agreement between FFT-based staging and conventional blood pressure (BP) classification
Treatment-naïve cohort design	Spectral changes reflect genuine early remodeling, unconfounded by pharmacotherapy
Wearable platform validation confirmed	Scalable deployment in frontline and resource-limited settings is feasible
Transparent composite index not a black-box model	Supports clinical adoption, regulatory review, and shared decision-making

Table 6
Comparison of recent AI-ECG studies for hypertension detection

Study	Year	Cohort characteristics	Classification	Model type	Key performance/distinctive features
Liang et al.	2025	Mixed treated and untreated	Binary + early heart change	Deep learning	High sensitivity for early hypertension-mediated change
Al-Alusi et al.	2025	Large mixed population	Binary hypertension (HTN) + cardiovascular (CV) risk	Deep learning	Digital biomarker approach; strong binary performance
Present study	2026	341 fully treatment-naïve patients	Four-category severity staging + binary	Transparent composite spectral index (Random Forest weighting)	88% 4-class accuracy ($\kappa = 0.868$); 95% binary accuracy; ROC-AUC 0.978; wearable validation; single 15-*s* recording

capture the same clinical severity gradient as conventional sphygmomanometry. The treatment-naive study design ensures that spectral changes reflect incipient myocardial remodeling rather than treatment effects. Taken together, these findings support single-encounter spectral ECG as a scalable, interpretable tool for early hypertension detection, risk stratification, and longitudinal monitoring. Recent AI-ECG studies relevant to hypertension detection are summarized in Table 6.

Table 6 places the present work in the context of recent AI-ECG hypertension studies. Most previous work has focused on binary classification in mixed (treated and untreated) populations using deep-learning models. In contrast, the current study examines a fully treatment-naive cohort, provides four-category severity staging, and employs a transparent composite index that remains fully interpretable.

The demographic characteristics of the full recruited cohort are provided in Appendix (Table S1).

9. Clinical Implications

Frequency-domain ECG analysis using a transparent regression-based composite index offers a practical single-encounter alternative to the multi-visit blood pressure measurement protocols mandated by current international guidelines. From a single 15-second high-resolution 12-lead recording, the method achieved 95% accuracy and 99% sensitivity for binary hypertension detection, and 88% accuracy across four clinically graded severity categories, with a weighted ROC-AUC of 0.978 and all misclassifications limited to adjacent groups.

A particularly significant clinical dimension of this approach is its capacity to identify spectral signatures of early, potentially reversible myocardial remodeling before overt structural changes become evident on echocardiography or cardiac MRI. This detection at a pre-structural stage preserves the intervention window during which concentric remodeling remains reversible, a window that closes with progression to established hypertrophy. By enabling earlier triage and treatment initiation, spectral ECG analysis may help prevent progression to irreversible hypertension-mediated organ damage.

The reproducibility of all spectral indices on Sydäntek wearable recordings confirms that deployment is not limited to supervised laboratory settings. The transparent, non-black-box architecture of the composite index further facilitates clinical adoption, supporting shared decision-making between clinicians and patients in a way that opaque deep-learning models cannot. The principal clinical implications of these findings are summarized in Table 5.

10. Learning Points

1) This study demonstrates that frequency-domain ECG analysis provides a rapid, single-encounter staging tool for

hypertension, offering a reproducible and interpretable alternative to the repeated blood pressure measurements currently required by international guidelines.
2) FFT-derived spectral features including total power, centroid frequency, and spectral resonance peak ratio achieved high accuracy and strong concordance with blood pressure-based severity classification (AUC >0.97, κ >0.83), validating their reliability as noninvasive surrogates for spectral signatures consistent with early myocardial involvement.
3) The binary classification model's 95% accuracy and 99% sensitivity for high-risk detection establish a strong evidence base for integration into frontline triage and population-level hypertension screening programs.

11. Innovation Statement

This study introduces a rapid-deployment spectral ECG platform (Sydäntek) capable of staging hypertension severity from a single 15-second recording using transparent FFT-based pattern recognition. In contrast to the multi-visit blood pressure measurement protocols embedded in current guidelines, this approach requires only brief chest contact and a single clinical encounter yielding an immediately interpretable, quantitative risk score. By combining multiple spectral features into a weighted composite index rather than relying on any single threshold, the system achieves clinically meaningful staging accuracy while remaining fully auditable. This positions spectral ECG as a scalable tool for earlier detection of hypertensive myocardial remodeling and a meaningful reduction in diagnostic burden across frontline and resource-limited practice environments.

12. Patient Perspective/Technician's Voice

As a participant and a nurse, I found the 15-second ECG recording far less cumbersome than the repeated visits required for conventional blood pressure monitoring. The device produced an immediate, interpretable risk score, and I appreciated that the diagnostic output drew on multiple complementary spectral features rather than a single measurement. From both a patient and a clinical perspective, this approach felt efficient, transparent, and well-suited to real-world hypertension staging.

13. Clinical Perspective

What is new?

This study demonstrates for the first time that a transparent, regression-based spectral composite index derived from a single 15-second high-resolution 12-lead ECG can accurately stage hypertension severity across four clinically defined categories in a treatment-naive cohort. Binary classification reached 95% accuracy with an ROC-AUC of 0.978, and wearable validation on the Sydäntek platform confirmed reproducibility within regulator-ready acquisition workflows.

What is relevant?

A single 15-second ECG recording can now deliver immediate, quantitative hypertension risk stratification across four severity grades. This enables earlier clinical triage, reduces the number of visits required before treatment initiation, and supports longitudinal compliance tracking through serial spectral scoring. At scale, this approach has the potential to fundamentally reshape hypertension screening strategy in both primary care and resource-limited settings.

Funding Support

This study was conducted as part of the institutional research and development initiatives of the Sydäntek wearable ECG platform at SJICR, Bengaluru, India. The high-resolution ECG acquisition system and signal processing infrastructure were supported by the National Biopharma Mission, BIRAC, Government of India. No specific funding was received for this particular study, and no commercial funding was involved.

Ethical Statement

The study was approved by the Institutional Ethics Committee of SJICR (SJICR/EC/2020/028). All participants provided written informed consent, and the study was conducted in accordance with the Declaration of Helsinki.

Conflicts of Interest

Dr Sugandhi Gopal, the principal investigator, served as both system designer and study director; this dual role is disclosed, governance measures minimized bias, and all underlying data are available for review to ensure transparency and reproducibility. The investigator's primary professional role is as an Interventional cardiologist, with research activities conducted in alignment with that clinical focus.

Mr Vishwateja Reddy (research associate in clinical trials design and monitoring) and Mr V. Harish (machine learning engineer) are affiliated with Carditek Medical Devices and contributed to this project in roles specific to signal processing and algorithm development. Their contributions were purely technical in nature and did not influence the study's clinical design, data interpretation, or outcome analysis. Dr Prabhavathi Bhat, Dr V. J. Karthikeyan, and Shasha Jumbe served as independent reviewers and proofreaders for the manuscript and declared no conflict of interest.

All contributors affirm adherence to ethical research practices and confirm that their roles did not introduce bias or commercial influence into the study's execution, analysis, or reporting.

Data Availability Statement

Data are available from the corresponding author upon reasonable request.

Author Contribution Statement

Sugandhi Gopal: Conceptualization, Methodology, Writing – original draft, Visualization, Supervision. **Prabhavathi Bhat:** Writing – review & editing, Supervision, Project administration. **V. J. Karthikeyan:** Writing – review & editing, Project administration. **Shasha Jumbe:** Writing – review & editing, Supervision. **Vishwateja Reddy:** Investigation, Data curation. **V. Harish:** Software, Validation, Formal analysis, Data curation.

References

[1] Kario, K., Okura, A., Hoshide, S., & Mogi, M. (2024). The WHO Global report 2023 on hypertension warning the

emerging hypertension burden in globe and its treatment strategy. *Hypertension Research*, *47*(5), 1099–1102. https://doi.org/10.1038/s41440-024-01622-w

[2] Whelton, P. K., Carey, R. M., Aronow, W. S., Casey, D. E., Jr., Collins, K. J., Dennison Himmelfarb, C., . . . , & Wright, J. T., Jr. (2018). 2017 ACC/AHA/AAPA/ABC/ACPM/AGS/APhA/ASH/ASPC/NMA/PCNA guideline for the prevention, detection, evaluation, and management of high blood pressure in adults: A report of the American College of Cardiology/American Heart Association Task Force on Clinical Practice Guidelines. *Hypertension*, *71*(6), e13–e115. https://doi.org/10.1161/HYP.0000000000000065

[3] Carey, R. M., Wright, J. T., Jr., Taler, S. J., & Whelton, P. K. (2021). Guideline-driven management of hypertension: An evidence-based update. *Circulation Research*, *128*(7), 827–846. https://doi.org/10.1161/CIRCRESAHA.121.318083

[4] Lee, E. K., Poon, P., Yip, B. H., Bo, Y., Zhu, M.-T., Yu, C.-P., . . . , & Wong, S. Y. (2022). Global burden, regional differences, trends, and health consequences of medication nonadherence for hypertension during 2010 to 2020: A meta-analysis involving 27 million patients. *Journal of the American Heart Association*, *11*(17), e026582. https://doi.org/10.1161/JAHA.122.026582

[5] Cook, D. A., Oh, S.-Y., & Pusic, M. V. (2020). Accuracy of physicians' electrocardiogram interpretations: A systematic review and meta-analysis. *JAMA Internal Medicine*, *180*(11), 1461–1471. https://doi.org/10.1001/jamainternmed.2020.3989

[6] Gopal, S., Bhat, P., Sivaram, S., Karthikeyan, V. J., Prabhu, M., Subramanian, M., . . . , & Srinivasan, A. (2025). From wires to wearables (1): Clinical equivalence with an axis-aware validation of a wearable ECG system (Sydäntek) with compressed lead geometry. *Smart Wearable Technology. Advance online publication*. https://doi.org/10.47852/bonviewSWT52026869

[7] Gopal, S., Bhat, P., Sivaram, S., Prabhu, M., Karthikeyan, V. J., Roy, P., . . . , & Subramanya, I. (2025). From wires to wearables (2): Temporal fidelity assessment of the Sydäntek wearable ECG system against a legacy cloud-based standard. *Smart Wearable Technology. Advance online publication*. https://doi.org/10.47852/bonviewSWT52027014

[8] Gopal, S., Bhat, P., Jumbe, S., Subramanian, M., Reddy, V., & Roy, P. (2026). From wires to wearables (3): ST-segment fidelity across modalities: Sydäntek's algorithmic transition from legacy leads to wearables. *Smart Wearable Technology. Advance online publication*. https://doi.org/10.47852/bonviewSWT62027971

[9] Kumar, M., A, & Chakrapani, A. (2022). Classification of ECG signal using FFT based improved Alexnet classifier. *PLoS ONE*, *17*(9), e0274225. https://doi.org/10.1371/journal.pone.0274225

[10] Liang, C., Yang, F., Huang, X., Zhang, L., & Wang, Y. (2025). Deep learning assists early-detection of hypertension-mediated heart change on ECG signals. *Hypertension Research*, *48*(2), 681–692. https://doi.org/10.1038/s41440-024-01938-7

[11] Singh, A. K., & Krishnan, S. (2023). ECG signal feature extraction trends in methods and applications. *BioMedical Engineering OnLine*, *22*(1), 22. https://doi.org/10.1186/s12938-023-01075-1

[12] Pedregosa, F., Varoquaux, G., Gramfort, A., Michel, V., Thirion, B., Grisel, O., . . . , & Duchesnay, É. (2011). Scikit-learn: Machine learning in Python. *Journal of Machine Learning Research*, *12*(85), 2825–2830.

[13] Pham, H., Egorov, K., Kazakov, A., & Budennyy, S. (2023). Machine learning-based detection of cardiovascular disease using ECG signals: Performance vs. complexity. *Frontiers in Cardiovascular Medicine*, *10*, 1229743. https://doi.org/10.3389/fcvm.2023.1229743

[14] Yang, J., & Yan, R. (2020). A multidimensional feature extraction and selection method for ECG arrhythmias classification. In *IEEE Sensors Journal*, *21*(13), 14180–14190. https://doi.org/10.1109/JSEN.2020.3047962

[15] Sharma, A., Tanwar, R. S., Singh, Y., Sharma, A., Daudra, S., Singal, G., . . . , & Pancholi, S. (2022). Heart rate and blood pressure measurement based on photoplethysmogram signal using fast Fourier transform. *Computers and Electrical Engineering*, *101*, 108057. https://doi.org/10.1016/j.compeleceng.2022.108057

[16] Sörnmo, L., & Laguna, P. (2005). *Bioelectrical signal processing in cardiac and neurological applications*. USA: Academic Press. https://doi.org/10.1016/B978-0-12-437552-9.X5000-4

[17] Unger, T., Borghi, C., Charchar, F., Khan, N. A., Poulter, N. R., Prabhakaran, D., . . . , & Schutte, A. E. (2020). 2020 International Society of Hypertension global hypertension practice guidelines. *Hypertension*, *75*(6), 1334–1357. https://doi.org/10.1161/HYPERTENSIONAHA.120.15026

[18] Williams, B., Mancia, G., Spiering, W., Rosei, E. A., Azizi, M., Burnier, M., . . . , & Desormais, I. (2018). 2018 ESC/ESH Guidelines for the management of arterial hypertension: The task force for the management of arterial hypertension of the European Society of Cardiology and the European Society of Hypertension. *Journal of Hypertension*, *36*(10), 1953–2041. https://doi.org/10.1097/HJH.0000000000001940

[19] Sau, A., Barker, J., Pastika, L., Sieliwonczyk, E., Patlatzoglou, K., McGurk, K. A., . . . , & Ng, F. S. (2025). Artificial intelligence-enhanced electrocardiography for prediction of incident hypertension. *JAMA Cardiology*, *10*(3), 214–223. https://doi.org/10.1001/jamacardio.2024.4796

[20] Liu, F., Xia, S., Wei, S., Chen, L., Ren, Y., Ren, X., . . . , & Liu, C. (2022). Wearable electrocardiogram quality assessment using wavelet scattering and LSTM. *Frontiers in Physiology*, *13*, 905447. https://doi.org/10.3389/fphys.2022.905447

How to Cite: Gopal, S., Bhat, P., Karthikeyan, V. J., Jumbe, S., Reddy, V., & Harish, V. (2026). Frequency-Domain ECG Analysis Enables Single-Encounter Hypertension Staging and Early Myocardial Remodeling Detection: A Prospective 384-Patient Study. *Smart Wearable Technology*. https://doi.org/10.47852/bonviewSWT620210590

Appendix

Table S1
Demographic table

Variable	Normal (n = 117)	Borderline/mild (n = 116)	Moderate (n = 91)	Severe (n = 60)	Overall (n = 384)
Age, years, mean ± SD	54.4 ± 14.4	52.8 ± 15.6	56.1 ± 14.2	56.6 ± 15.0	54.6 ± 14.8
Age range, years	22–86	17–89	25–84	20–85	17–89
Male, n (%)	49 (41.9)	71 (61.2)	59 (64.8)	40 (66.7)	219 (57.0)
Female, n (%)	68 (58.1)	45 (38.8)	32 (35.2)	20 (33.3)	165 (43.0)
BMI, kg/m², mean ± SD	26.8 ± 3.5	25.7 ± 4.4	25.6 ± 4.9	27.5 ± 4.3*	26.3 ± 4.3
Office SBP, mmHg, mean ± SD	118.5 ± 8.4	130.8 ± 5.6	153.9 ± 3.8	184.6 ± 10.6	—
Office DBP, mmHg, mean ± SD	71.2 ± 6.4	86.4 ± 2.8	95.8 ± 2.1	122.5 ± 10.9	—

In this cohort, age was not associated with hypertension grade, and BMI showed no monotonic relationship with severity. Male sex was more frequent in the hypertensive categories than in the normotensive group. Age, sex, and BMI were not used as inputs to the spectral composite index. A brief statement to this effect has been added at the beginning of the results.